



Magnetic evidence of anthropogenic dust deposition in urban soils of Shanghai, China



Guan Wang^{a,b}, Feifan Ren^c, Jiao Chen^a, Yuan Liu^d, Fangzhou Ye^d, Frank Oldfield^e, Weiguo Zhang^b, Xiaodong Zhang^{a,*}

^a School of Environment and Architecture, University of Shanghai for Science and Technology, Shanghai 200093, China

^b State Key Laboratory of Estuarine and Coastal Research, East China Normal University, Shanghai 200062, China

^c Key Laboratory of Geotechnical and Underground Engineering of the Ministry of Education, Tongji University, Shanghai 200092, China

^d Department of Geography, East China Normal University, Shanghai 200062, China

^e School of Environmental Sciences, University of Liverpool, Liverpool, UK

ARTICLE INFO

Article history:

Received 18 March 2016

Received in revised form 27 March 2017

Accepted 14 July 2017

Editorial handling - Stefan Norra

Keywords:

Soil
Magnetic properties
Pollution
Shanghai

ABSTRACT

The magnetic particulates from anthropogenic activities can be detected by magnetic methods rapidly and cost-effectively. This study focused on the investigation of vertical variations in magnetic properties in soil profiles and magnetic enhancement originating in Baoshan, Shanghai. Also the feasibility of using arable and urban park soils as a new context for magnetic monitoring was explored. A combination of magnetic and scanning electron microscopic (SEM) techniques was applied to three soil profiles. Non-pedogenic magnetic enhancement in topsoil was recorded at all three sites accompanied by coarsening of magnetic grain size. The dominant magnetic properties reflect multi-domain (MD) and pseudo-stable single domain (PSD) ferrimagnetic minerals. Both of magnetic concentrations and grain size decrease with the depth, depending on the pollutant input, soil type and degree of vertical mixing. SEM images confirmed the presence of anthropogenic particulates fly-ash. It was concluded from this study that topsoil magnetic enhancement arising from atmospheric contaminants was readily identifiable in both arable fields and urban parks, thus broadening the scope of magnetic research on urban and industrial pollution.

© 2017 Elsevier GmbH. All rights reserved.

1. Introduction

Magnetic enhancement of topsoil is caused by either natural pedogenic, or anthropogenic (industrial dust, vehicle exhaust and other atmospheric pollutant) processes. The anthropogenic impact on soil profiles can be easily separated from pedogenic enhancement (Lecoanet et al., 2003; Magiera and Zawadzki, 2007; Blaha et al., 2008; Blundell et al., 2009; Kim et al., 2009; Łukasik et al., 2014), since anthropogenic magnetic particles are characterized by specific morphology and coarser magnetic grain size compared with the fine-grained superparamagnetic (SP) and single domain (SD) grains of pedogenic origin (Mullins, 1977; Lecoanet et al., 2001; Ska et al., 2004; Fialov et al., 2006; Lu and Bai, 2006; Magiera et al.,

2006; Magiera et al., 2007; Blaha et al., 2008; Magiera et al., 2008; Muxworthy et al., 2002; Łukasik et al., 2014).

Owing to the significant correlation between magnetic susceptibility (MS) and heavy metal contamination in soils (Georgeaud et al., 1997; Xie et al., 2001; Robertson et al., 2003; Desenfant et al., 2004; Gautam et al., 2005; Lu et al., 2007; Yang et al., 2014), non-destructive and rapid magnetic techniques have been increasingly used to detect environmental pollution of soils, sediments and dusts in many studies (Hay et al., 1997; Strzyszc and Magiera, 1998; Moreno et al., 2003; Boyko et al., 2004; Fialov et al., 2006; Lu and Bai, 2006; Blaha et al., 2008; Sharma and Tripathi, 2008; Zhang et al., 2008; Blundell et al., 2009; Morton-Bermea et al., 2009; Wang et al., 2008; Wang et al., 2012; Pietrodangelo et al., 2013; Yang et al., 2014).

With the rapid industrialization and urbanization, dust pollution is a widespread phenomenon in urban areas. As a result, farmland and parkland soils around industrial areas and transportation lines are becoming increasingly susceptible to atmospherically derived pollution, which may pose serious threats to

* Corresponding author at: School of Environment and Architecture, University of Shanghai for Science and Technology, Shanghai 200093, China.
E-mail address: fatzhxd@126.com (X. Zhang).

food production and human health. Due to the up-to-down migration characteristics of the dust pollution in the topsoil, the study on soil profiles can provide information on anthropogenic dust input, which may be useful for pollution control and management.

Baoshan District, an industrial zone surrounded by arable land in Shanghai, has suffered varying amounts of soil pollution by a wide range of metal concentrations. Hu et al. (2007) reported that the magnetic susceptibility (MS) of topsoils in Baoshan was significantly correlated with heavy metal concentrations. However, few studies on soil profile pollution have been reported. In addition to magnetic susceptibility, additional magnetic parameters can provide detailed information on magnetic particles in terms of concentration, grain size and type. The aims of the present study are to investigate how magnetic properties vary with soil depth and land use, and to explore their linkage to atmospheric dust input.

2. Samples and methods

2.1. Study area and samples

Located in the northern part of Shanghai city (Fig. 1), Baoshan District, has also been heavily affected by rapid urbanization in recent years. In this district, many heavy industries are sited, such as, Baosteel, Shanghai No. 1 Iron and Steel Company, Shanghai Ferroalloy Company, Shanghai Chemical Plant, Shanghai Cement Plant, Shanghai Iron Smelting Plant. The predominant wind direction in this region is northeast in winter and southeast in summer. The land in Baoshan District mainly locates on the deltaic deposits of the Yangtze River Estuary, and may be classified as Entisols (Hu et al., 2007). In order to study the impacts of urbanization and industrial airborne particulate matter on the soil environment, three short soil cores (40 cm in length) were collected from Linjiang Park (LJ), Yuepu Park (YP) and arable land (AL), respectively (Fig. 1). To prevent any possible contamination, the outer ring of the core was removed before subsampling. The soil cores were sectioned at 2 cm interval, and the samples were oven dried at 40 °C before laboratory analysis.

2.2. Methods

2.2.1. Magnetic measurement

About 4–5 g soil was packed tightly into 8 ml plastic boxes and fixed for routine isothermal magnetic measurements. MS (χ) was measured on samples at low frequency (0.47 kHz) (χ_{lf}) and high frequency (4.7 kHz) (χ_{hf}) using a Bartington MS2 meter. Anhyseretic Remanent Magnetization was induced in a steady field of 0.04 mT imposed on a peak AF field of 100 mT using a DTECH 2000 demagnetizer. Values have been normalized for the DC bias field and expressed as χ_{ARM} . Isothermal Remanent Magnetization (IRM) was grown in fields of 1 T, –100 mT and –300 mT using a Molspin pulse magnetizer and all remanences were measured in a Molspin low-speed spinner magnetometer. Magnetic hysteresis loops and Curie Temperatures were measured on selected samples using a variable field translation balance (Petersen Instruments, MMvftb). Magnetic parameters are expressed as mass-specific values and inter-parametric quotients have also been calculated in order to give quantitative and qualitative information of magnetic particulates. The properties recorded include MS (χ_{lf}), χ_{ARM} , SIRM (SIRM = IRM_{1000mT}), HIRM (HIRM = [(SIRM + IRM₋₃₀₀)/2]), $\chi_{fd}\%$ ($\chi_{fd}\% = [\chi_{lf} - \chi_{hf}] / \chi_{lf} \times 100$), χ_{ARM} / χ_{lf} , χ_{ARM} / SIRM , SIRM/ χ_{lf} and S-ratio (IRM₋₃₀₀/SIRM). The magnetic susceptibility χ_{lf} indicates the total contribution of magnetic minerals represented by the concentration of ferrimagnetic minerals in the sample. χ_{ARM} and SIRM are also magnetic parameters related to magnetic minerals concentrations. HIRM estimates antiferromagnetic components in a sample. $\chi_{fd}\%$ relates to the superparamagnetic (SP) ferrimagnetic component, while χ_{ARM} / χ_{lf} , χ_{ARM} / SIRM ratios can indicate ferrimagnetic minerals grain size. SIRM/ χ_{lf} and S-ratios are often employed as grain size and type indicators for magnetic minerals. Further information on the interpretation of these measurements and quotients can be found in Chen et al. (Chen et al., 1995) and Walden et al. (Walden et al., 1999).

2.2.2. SEM analysis

For each soil profile, three samples from the top, middle and bottom part of the core were selected for SEM (Scanning Electronic

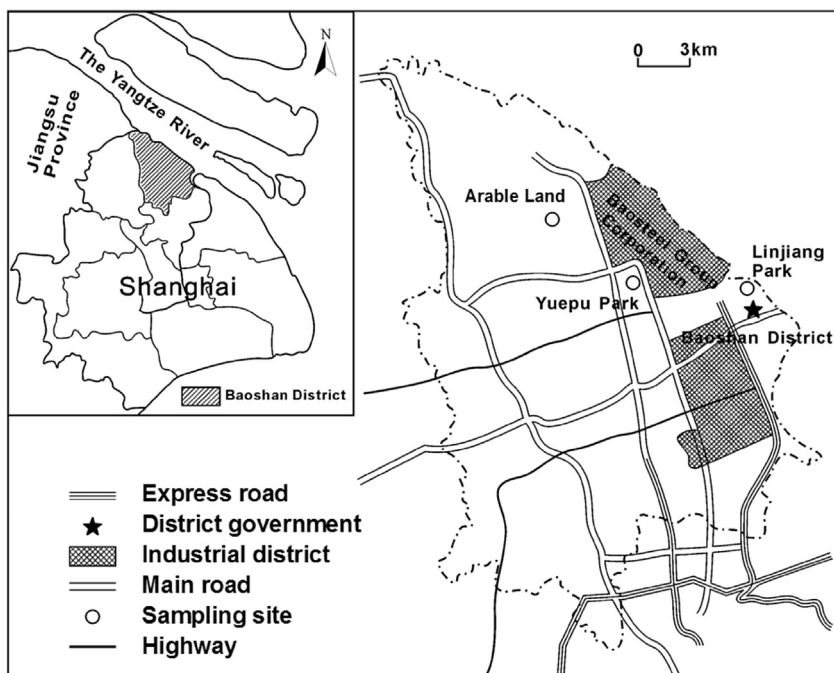


Fig. 1. Maps of Shanghai and soil core sampling.

Table 1
Magnetic properties of the urban and agricultural soils in Baoshan District, Shanghai.

| Parameters (unit) | Background | Linjiang Park | | Yuepu Park | | Arable land | |
|---|------------|---------------|-------|--------------|--------|--------------|-------|
| | | Range | Mean | Range | Mean | Range | Mean |
| χ_{if} ($10^{-8} \text{ m}^3 \text{ kg}^{-1}$) | 30.6 | 42.4–120.5 | 64.2 | 29.7–116.5 | 60.3 | 12.4–78.1 | 31.0 |
| χ_{ARM} ($10^{-8} \text{ m}^3 \text{ kg}^{-1}$) | 134.9 | 177.4–373.9 | 242.6 | 102.8–222.9 | 160.79 | 54.2–238.5 | 122.8 |
| SIRM ($10^{-5} \text{ Am}^2 \text{ kg}^{-1}$) | 398.1 | 555.8–1638.9 | 850.4 | 410.4–1518.4 | 789.32 | 140.4–1064.8 | 395.8 |
| HIRM ($10^{-5} \text{ Am}^2 \text{ kg}^{-1}$) | 31.4 | 32.2–65.1 | 39.9 | 22.3–58.7 | 33.01 | 26.8–56.9 | 34.3 |
| $\chi_{fd}\%$ | 2.2 | 2.4–6.3 | 3.8 | 0.3–4.2 | 2.07 | –3.2–4.8 | 1.4 |
| SIRM/ χ_{if} (kAm^{-1}) | 12.7 | 12.3–14.7 | 13.2 | 10.2–15.0 | 13.13 | 10.2–15.1 | 12.2 |
| χ_{ARM}/χ_{LF} | 4.4 | 3.1–5.0 | 3.9 | 1.9–4.9 | 3.10 | 3.0–5.8 | 4.4 |
| χ_{ARM}/SIRM (10^{-3} mA^{-1}) | 0.4 | 0.2–0.4 | 0.3 | 0.2–0.4 | 0.24 | 0.2–0.5 | 0.4 |
| S-ratio | 0.78 | 0.86–0.94 | 0.9 | 0.86–0.95 | 0.91 | 0.57–0.95 | 0.75 |

Microscopy) analysis. The magnetic components were extracted using a hand magnet. SEM analysis was carried out with a JEOL JSM-5610LV equipped with an energy dispersive x-ray (EDS) analysis system,

3. Results and discussion

3.1. Magnetic properties of the soil profile

3.1.1. Magnetic mineral content

The magnetic properties of the soil cores are summarized in Table 1, and with their vertical variations are shown in Fig. 2. MS (χ_{if}) indicates approximately the total contribution of

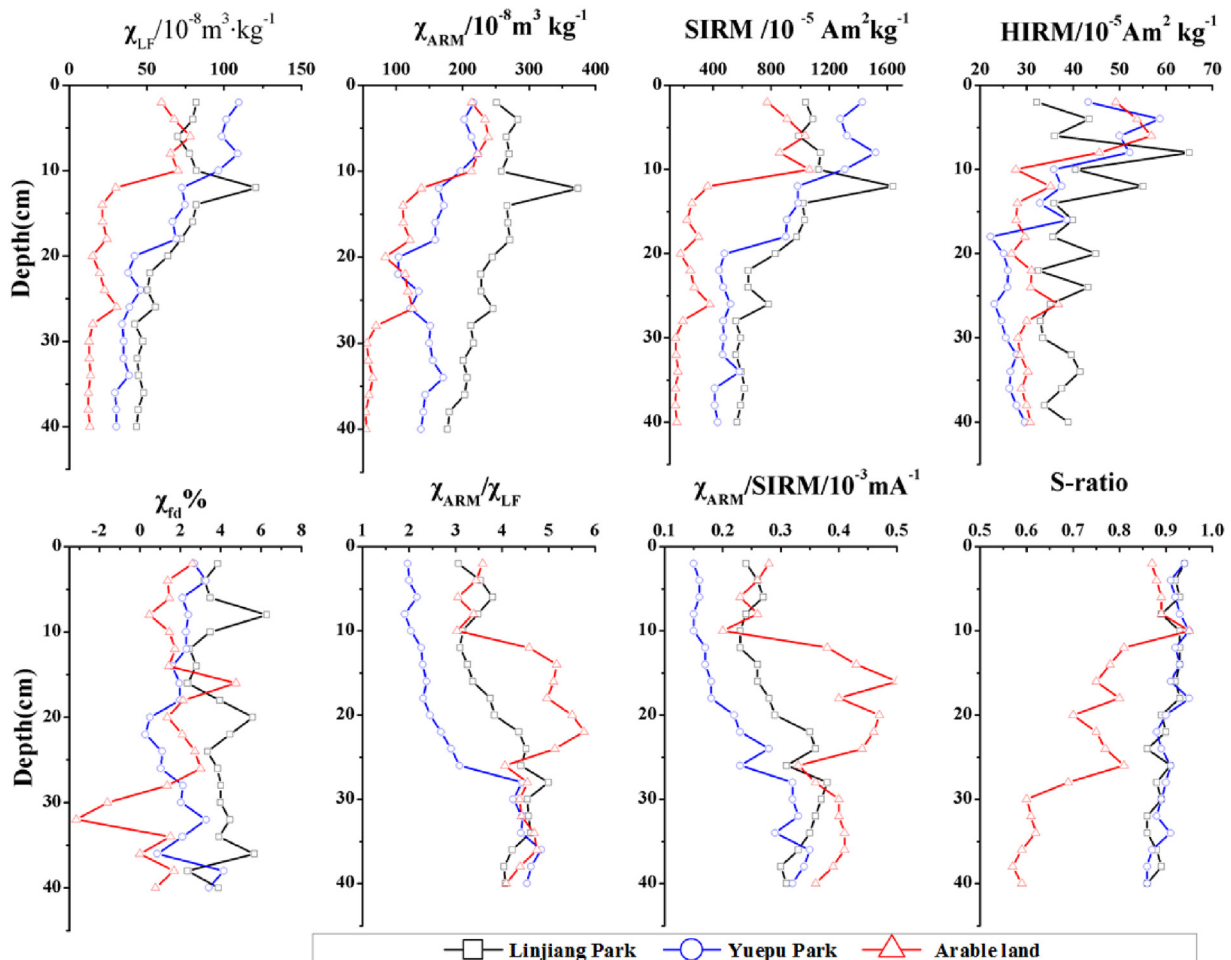


Fig. 2. Vertical distribution of magnetic properties in soil profile.

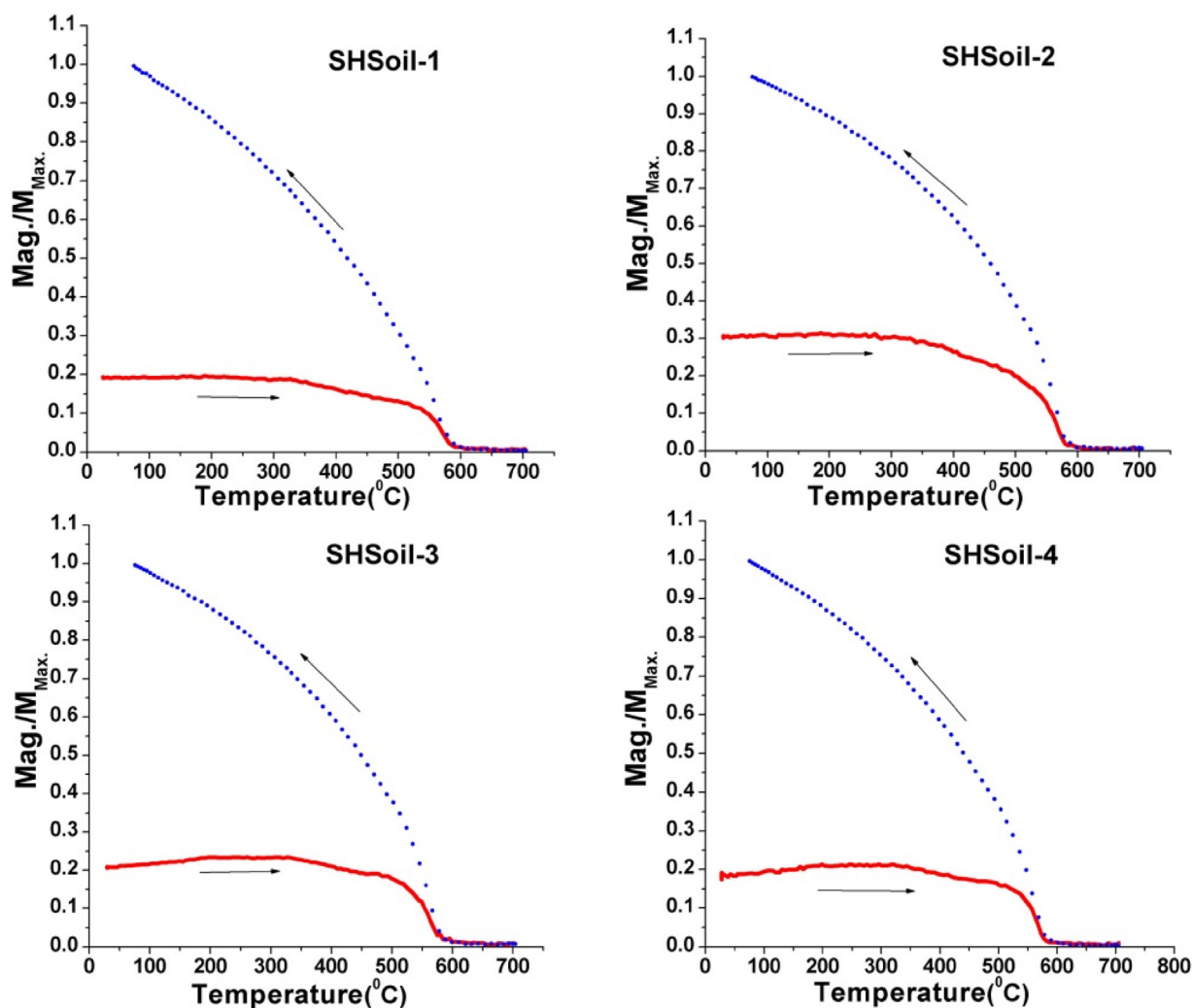


Fig. 3. Thermomagnetic curves of selected Shanghai Baoshan soil samples.

magnetic minerals (mainly ferrimagnetic minerals such as magnetite) in the sample (Thompson and Oldfield, 1986). It ranges from $12.36 \times 10^{-8} \text{ m}^3 \text{ kg}^{-1}$ to $120.52 \times 10^{-8} \text{ m}^3 \text{ kg}^{-1}$ with an average of $51.80 \times 10^{-8} \text{ m}^3 \text{ kg}^{-1}$. All the three soil profiles (Fig. 2) show noticeable magnetic enhancement in the uppermost layer (0–20 cm). The samples from 0 to 10 cm have the highest MS values. The samples from 10 to 20 cm still show relative high MS values compared with the lower horizons, but not as high as in the uppermost soil layers. The magnetic susceptibilities in the basal horizons (20–40 cm) are relatively constant and have the lowest values.

The low and homogeneous MS values in the lower part can be considered as the background values (Table 1), and the values was found to be $44.46 \times 10^{-8} \text{ m}^3 \text{ kg}^{-1}$ for LJ, $33.24 \times 10^{-8} \text{ m}^3 \text{ kg}^{-1}$ for YP, $12.96 \times 10^{-8} \text{ m}^3 \text{ kg}^{-1}$ for AL, respectively. They are comparable with MS value of background soil in the district ($30.55 \times 10^{-8} \text{ m}^3 \text{ kg}^{-1}$), whilst the maximum MS values of the topsoil are about 4 times higher than the background values.

SIRM and χ_{ARM} are also concentration related magnetic parameters (Oldfield and Yu, 1994). SIRM is contributed largely by ferrimagnetic and antiferromagnetic minerals but not by paramagnetic and diamagnetic materials (Thompson and Oldfield, 1986), while χ_{ARM} is especially sensitive to the content of stable single domain (SD) ferrimagnetic grains (Maher, 1988). HIRM can provide a rough estimate of changes in the relative importance of antiferromagnetic components (mainly hematite) in a sample.

Mean values of SIRM and χ_{ARM} are $678.51 \times 10^{-5} \text{ Am}^2 \text{ kg}^{-1}$ and $175.39 \times 10^{-8} \text{ m}^3 \text{ kg}^{-1}$, respectively (Table 1). SIRM, χ_{ARM} and HIRM values all show similar variations to those for magnetic susceptibility (Fig. 2).

3.1.2. Magnetic mineralogy

The so-called S-ratio ($=\text{IRM}_{-300\text{mT}}/\text{IRM}_{1\text{T}}$) provides a measure of the relative contributions to IRM of high-coercivity (“hard”) remanence to low-coercivity (“soft”) remanence. Values close to unity indicate that the remanence is dominated by ‘soft’ ferrimagnets (Evans, 2003). The values of the S-ratio in the study area show that ferrimagnetic minerals dominate the magnetic properties of the magnetically enhanced topsoil, and higher concentrations of ferrimagnets exist in the urban park than in the arable land. Thermomagnetic curves on selected soil samples are shown in Fig. 3. The Curie temperature of 580°C indicates that magnetite is the main ferrimagnetic mineral. All the plots have cooling curves much higher than heating curves, suggesting the formation of new ferrimagnetic minerals during these cycles, presumably as a result of the presence of organic matter in the samples. Meanwhile, the significant correlations between χ_{lf} and SIRM and χ_{arm} (Table 2) in the soils also indicate the dominance of ferrimagnetic grains as the carrier of MS. It is important to note that dominance of the magnetic properties by magnetite does not reflect dominance of the mag-

Table 2The Spearman Correlation coefficients of χ_{lf} and other magnetic parameters for the soil samples in Baoshan.

| | Site | χ_{ARM} | SIRM | HIRM | $\chi_{fd}\%$ | SIRM/ χ_{lf} | χ_{ARM}/χ_{lf} | $\chi_{ARM}/SIRM$ | S-ratio |
|-------------|------|--------------|-----------|-----------|---------------|-------------------|------------------------|-------------------|-----------|
| χ_{lf} | LJ | 0.874(**) | 0.962(**) | 0.293 | -0.396 | 0.281 | -0.895(**) | -0.887(**) | 0.850(**) |
| | YP | 0.749(**) | 0.959(**) | 0.602(**) | 0.164 | -0.448(*) | -0.979(**) | -0.965(**) | 0.854(**) |
| | AL | 0.970(**) | 0.992(**) | 0.505(*) | 0.393 | 0.817(**) | -0.474(*) | -0.580(**) | 0.981(**) |

N=20 **. Correlation is significant at the 0.01 level (2-tailed).

*. Correlation is significant at the 0.05 level (2-tailed).

netic mineral assemblages, since hematite is under-represented in these measurements by around two orders of magnitude,

Four loops taken from both upper and lower layers of three sampling sites, show very similar hysteresis loops (Fig. 4). All the loops become closed below the field of 300 mT, and the samples have B_{cr} of less than 45 mT (Fig. 4) further confirming that magnetite dominates the magnetic properties.

3.1.3. Grain size of magnetic minerals

The magnetic parameter ratios can be used to infer magnetic grain size. Frequency-dependent susceptibility χ_{fd} reflects

the presence of grains at the transition between SP and SD and has often been used to approximate the importance of the superparamagnetic (SP) ferrimagnetic component (Dearing et al., 1996). Expressed as a percentage of χ_{lf} , $\chi_{fd}\%$ can help do distinguish between pedogenic and non-pedogenic ferrimagnetic assemblages. The low $\chi_{fd}\%$ values of the surface samples (all but one <4%) confirm that fine pedogenic grains contribute little to the magnetic enhancement of the profiles studied (Fig. 5).

$\chi_{ARM}/SIRM$ ratios can also indicate ferrimagnetic grain size, with the values decreasing with increasing grain size (Maher, 1988; Evans, 2003). $\chi_{arm}/SIRM$ values in the upper layers are signifi-

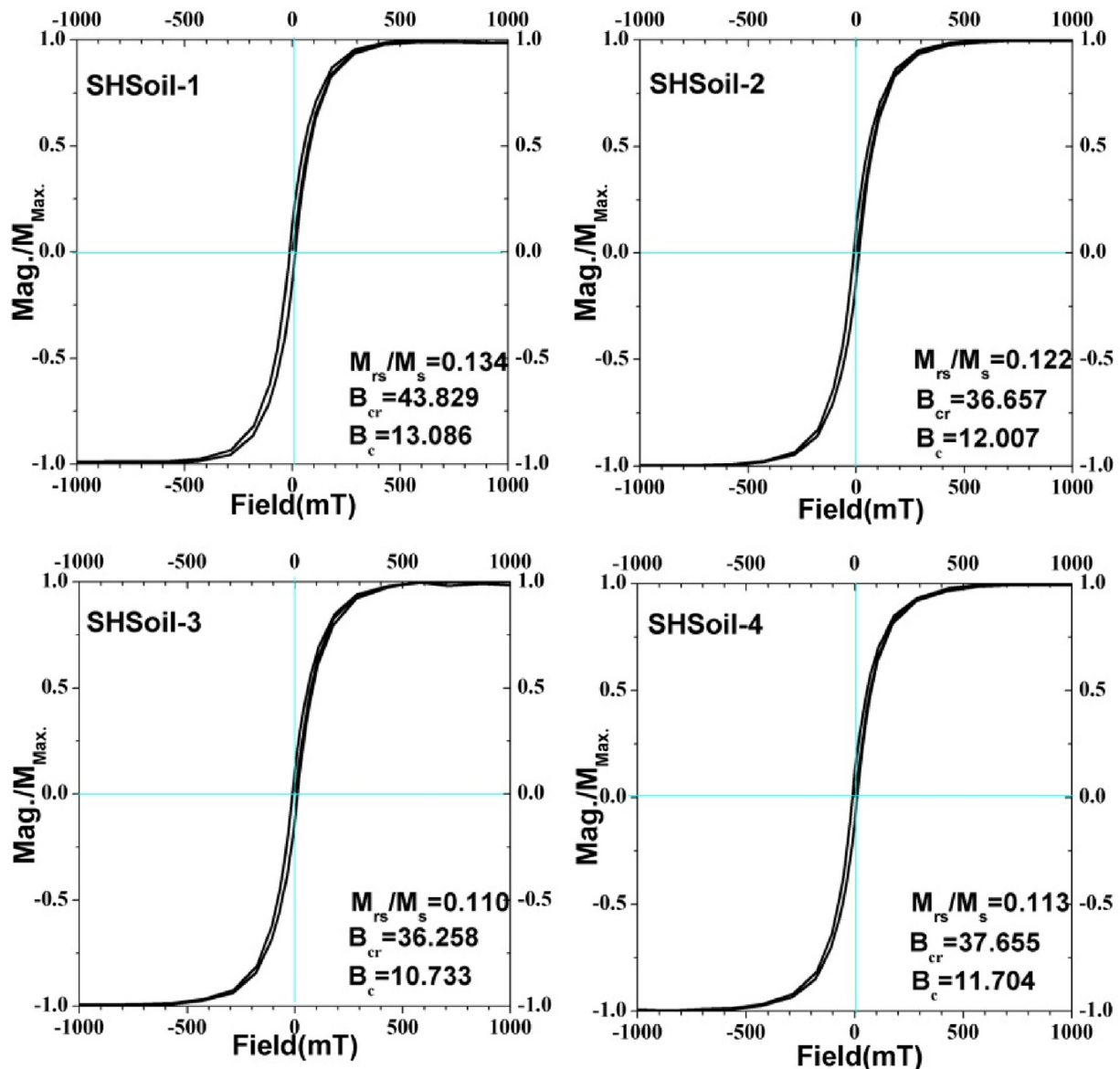


Fig. 4. Magnetic hysteresis loop with maximum field of 1.0T for representative soil samples collected from different soil layers.

cantly lower (Fig. 5), pointing to coarser magnetic grains in the urban (0–20 cm) topsoils. In magnetic assemblages where the dominant grain size is greater than SD, $\chi_{\text{ARM}}/\chi_{\text{IF}}$ also decreases with increasing grain size. The negative relationships between χ_{IF} and both $\chi_{\text{arm}}/\chi_{\text{IF}}$ and $\chi_{\text{arm}}/\text{SIRM}$ (Table 2), therefore confirm that the magnetic enhancement of the urban topsoil is caused by coarser magnetic particles. Mineral grains containing many domains are called multidomain (MD) particles; those containing only one are referred single-domain particles. The grains are MD which possess many of the properties of assemblages of true SD grains are referred pseudo-single-domain (PSD) particles. In addition, quotients derived from the hysteresis plots and shown in Fig. 4 are typical of PSD grains close to the PSD/MD border (Day et al., 1977) which is consistent with the position of the samples in Fig. 5 based on Dearing et al. (1997). It is assumed that SP grains block as fine SSD grains on the SP/SSD boundary ($\approx 0.030\text{--}0.040\ \mu\text{m}$), not as coarser SSD ($0.040\text{--}0.050\ \mu\text{m}$) or pseudo-single domain (PSD) grains ($0.050\text{--}8.000\ \mu\text{m}$) (Day et al., 1997). All these magnetic indicators confirm that the samples from the upper part of each profile are relatively coarser than the lower samples, confirming the view that atmospheric deposition of industrial/urban contaminants is the dominant source of the magnetic ‘enhancement’.

3.2. SEM analysis

The SEM analysis demonstrates the prevalence of magnetic spherical particles in the samples (Fig. 6). Such spherules are typical of industrial emissions from the high-temperature combustion of fossil fuels and have been illustrated in various publications (Hanesch et al., 2003; Blaha et al., 2008). Soil samples collected from the upper layers show a higher concentration of magnetic spherical particles and the particles are larger, with diameters ranging from ~ 40 up to $\sim 125\ \mu\text{m}$ (Fig. 6); whilst soil samples collected from lower part show few spherical particles except the sample in Yuepu Park (at $-38\ \text{cm}$ soil layer) (Fig. 6). EDS spectrum analysis indicates that the spherical particles are primarily composed of Fe and O with minor presence of Si and Al (Fig. 6).

In urban and industrial areas, the effect of topsoil susceptibility enhancement is obvious; however, the anthropogenic enhanced layers are quite different according to the land use type. χ_{IF} in the urban park topsoil is significantly higher than in the agricultural topsoil (Fig. 2). Here, the $\Sigma(\chi_{\text{IFi}} - \chi_{\text{IFo}})$ is used to estimate the total inventory of the ferrimagnetic input to the soil profiles in this study. χ_{IFi} is the measured MS value of each subsamples, while χ_{IFo} is the background MS value of each profile, obtained by calculating the average MS value below 30 cm in each case. The calculated values are $373.94 \times 10^{-8}\ \text{m}^3\ \text{kg}^{-1}$ (LJ), $532.58 \times 10^{-8}\ \text{m}^3\ \text{kg}^{-1}$ (YP) and $361.05 \times 10^{-8}\ \text{m}^3\ \text{kg}^{-1}$ (AL), respectively. All three sampling sites are close to the industrial area, but the arable site is much further from the residential district and high-density traffic lines than other two urban park sampling sites. The Yuepu Park site, located in the densely populated residential and business area with a viaduct nearby, is more impacted by anthropogenic activities than other two sampling sites. Thus, in addition to the influence of soil parent material and industrial pollution on magnetic enhancement, the effect of urban boilers, home hearths and the traffic emissions could also be significant contributors to magnetic enhancement. MS values at the arable land site are lower than the background value below 10 cm, while MS values in other two profiles are still slightly higher than the background value. This may reflect the effects of ploughing, soil type or the degree of pollution.

Magnetic enhancement as a result of atmospheric deposition has been recorded in many study areas (Hu et al., 2006; Magiera et al., 2006; Lu et al., 2007; Magiera et al., 2007; Duan et al., 2010). The depth, to which magnetic enhancement is recorded, may be useful as an indicator of the depth of penetration of other contam-

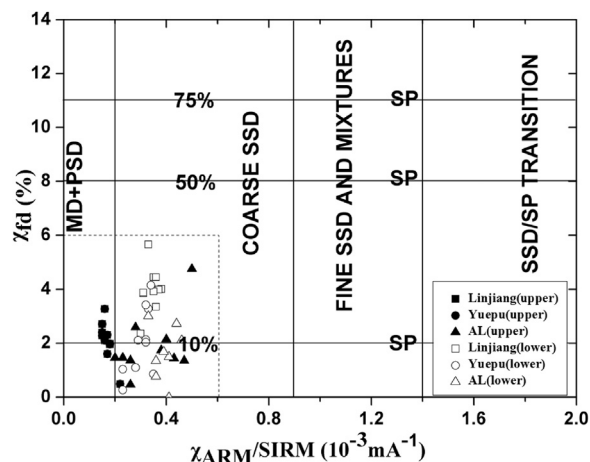


Fig. 5. Scatter diagram of $\chi_{\text{fd}}\%$ and $\chi_{\text{ARM}}/\text{SIRM}$ of soil profiles in Baoshan urban area.

inants. The low and stable magnetic concentrations below 20 cm are in accord with the studies of Magiera (Magiera et al., 2006).

However, the degree, to which the anthropogenically enhanced surface layers exceed the background values in the Chinese sites, is 30–80 times lower than in several published soil profiles from other countries (Hu et al., 2006; Magiera et al., 2006; Lu et al., 2007; Magiera et al., 2007; Duan et al., 2010). This may be the result of differences in parent material, the history of iron and steel production or the distance between the sampling sites and the plant.

Thus, magnetic and SEM/EDS analysis indicate that spherical particles rich in magnetite of coarse MD–PSD size make a significant contribution to the topsoil of the urban and arable fields in the Baoshan industrial district. These results confirm significant input from industrial activities and traffic emissions to each of the soil profiles studied.

4. Conclusions

This study illustrates a widely applicable approach for large-scale, high-resolution magnetic industrial pollution research in China, where it is often difficult to find the undisturbed soils in industrial districts. Nondestructive soil magnetic measurements can be rapidly carried out at low cost both in the field and laboratory, and it can be easily used to trace the extent of soil contamination in industrialized areas. The anthropogenic origin of magnetically enhanced topsoil MS in the study area has been confirmed by a series of diagnostic measurements.

The conclusions can be summarized as follows.

- (1) Anomalous magnetic enhancement is observed in the soil samples of the areas close to industrial or urban sources of pollution. The strongest enhancement of susceptibility is located within the uppermost 20 cm of each soil profile, and the magnetic concentrations of the soil below 20 cm are relatively stable and low.
- (2) Particles rich in relatively coarse MD–PSD magnetite dominate the magnetic properties of the surface soils, which can be concluded as a result of atmospheric deposition from vehicle exhausts, iron and steel works and domestic sources in the Baoshan District.
- (3) The SEM/EDS analysis demonstrates that magnetic spherules, which is prevalent in Baoshan district, result from the high-temperature combustion of fossil fuels. The SEM results confirm that the input of the particulates in all soil profiles is mainly derived from industries.

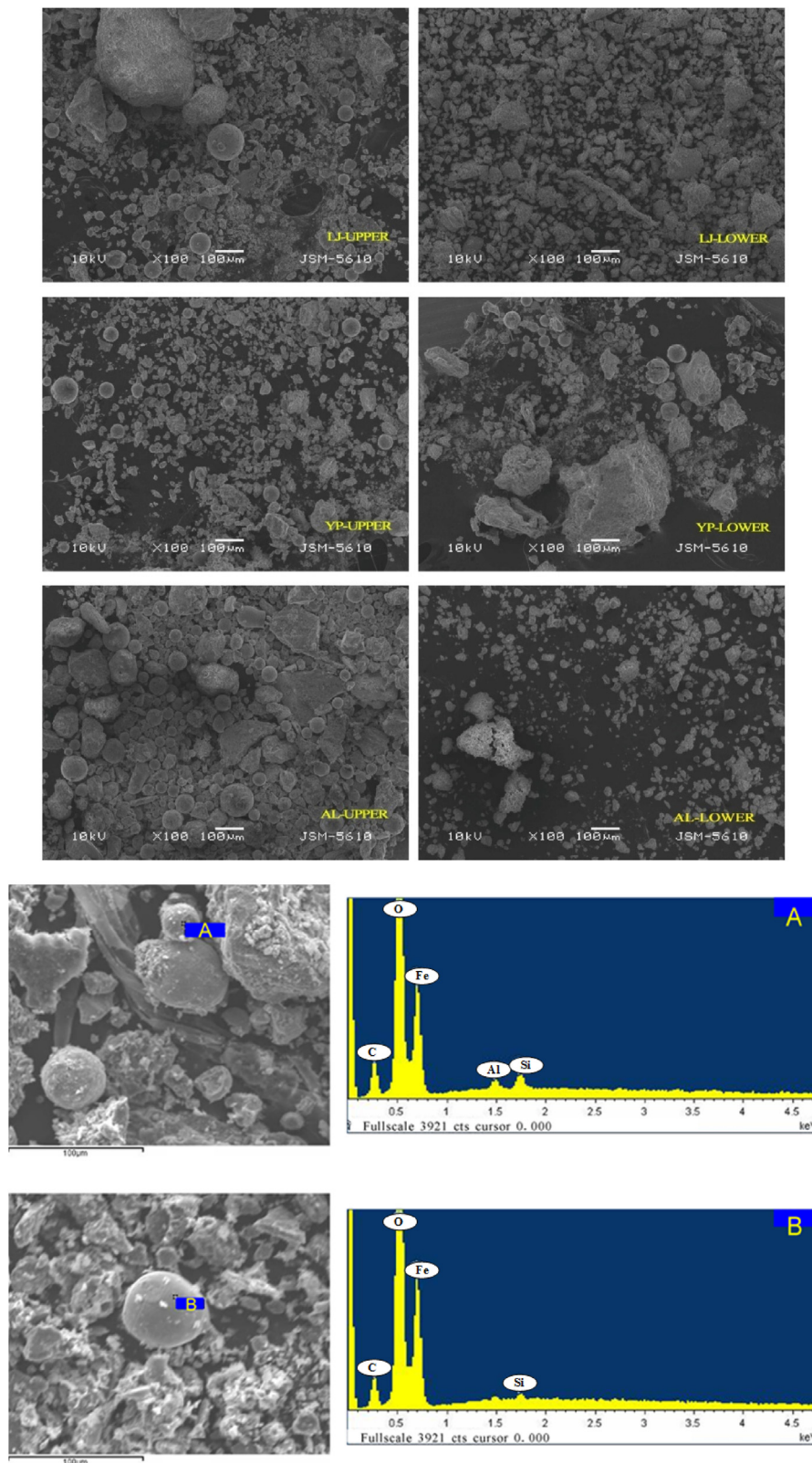


Fig. 6. SEM results and EDS spectra of extracted magnetic particles from three sampling sites.

- (4) Although it has been found in the previous studies that forest soils and other natural soil profiles can preserve more undisturbed information on the concentration and migration of magnetic minerals and heavy metals, arable soil and urban park soil can also be used in pollution monitoring, and atmospherically derived magnetic enhancement can be readily detected.

Acknowledgments

This study was supported by the National Natural Science Foundation of China (Grant No. 41001331), The Programme of Introducing Talents of Discipline to University (111 Project) and the Natural Science Foundation of Shanghai (Grant No.

15ZR1428700). The authors are grateful to Dr. Bing Ni in ECNU and Lecture Wang in Donghua University, Shanghai for their valuable help with SEM/EDS analysis, and to Limin Zhou in ECNU for geochemical analysis.

References

- Blaħa, U., Appel, E., Stanjek, H., 2008. Determination of anthropogenic boundary depth in industrially polluted soil and semi-quantification of heavy metal loads using magnetic susceptibility. *Environ. Pollut.* 156, 278–289.
- Blundell, A., Hannam, J.A., Dearing, J.A., Boyle, J.F., 2009. Detecting atmospheric pollution in surface soils using magnetic measurements: a reappraisal using an England and Wales database. *Environ. Pollut.* 157, 2878–2890.
- Boyko, T., Scholger, R., Stanjek, H., 2004. Topsoil magnetic susceptibility mapping as a tool for pollution monitoring: repeatability of in situ measurements. *J. Appl. Geophys.* 55, 249–259.
- Chen, F.H., Wu, R., Pompei, D., Oldfield, F., 1995. Magnetic property and particle size variations in late Pleistocene and Holocene parts of the Dadongling Loess Section near Xining, China. *Quat. Proc.* 4, 27–40.
- Dearing, J.A., Dann, R.J.L., Hay, K., Lees, J.A., Loveland, P.J., Maher, B.A., O'Grady, K., 1996. Frequency-dependent susceptibility measurements of environmental materials. *Geophys. J. Int.* 124, 228–240.
- Dearing, J.A., Bird, P.M., Dann, R.J.L., Benjamin, S.F., 1997. Secondary ferrimagnetic minerals in Welsh soils: a comparison of mineral magnetic detection methods and implications for mineral formation. *Geophys. J. Int.* 130, 727–736.
- Desenfant, F., Petrovsky, E., Rochette, P., 2004. Magnetic signature of industrial pollution of stream sediments and correlation with heavy metals: case study from South France. *Water Air Soil Pollut.* 152, 297–312.
- Duan, X., Hu, S., Yan, H., Blaħa, U., Roesler, W., Appel, E., Sun, W., 2010. Relationship between magnetic parameters and heavy element contents of arable soil around a steel company, Nanjing. *Sci. China Ser. D* 53, 411–418.
- Evans, M.E. (Ed.), 2003. *Environmental Magnetism—principles and Applications of Environmagnetics*. Academic Press.
- Fialov, H., Maier, G., Petrovsk, E., Kapicka, A., Boyko, T., Scholger, R., 2006. Magnetic properties of soils from sites with different geological and environmental settings. *J. Appl. Geophys.* 59, 273–283.
- Gautam, P., Blaħa, U., Appel, E., 2005. Magnetic susceptibility of dust-loaded leaves as a proxy of traffic-related heavy metal pollution in Kathmandu city, Nepal. *Atmos. Environ.* 39, 2201–2211.
- Georgeaud, V.M., Rochette, P., Ambrosi, J.P., Vandamme, D., Williamson, D., 1997. Relationship between heavy metals and magnetic properties in a large polluted catchment: The Etang de Berre (South of France). *Phys. Chem. Earth.* 22, 211–214.
- Hanesch, M., Scholger, R., Rey, D., 2003. Mapping dust distribution around an industrial site by measuring magnetic parameters of tree leaves. *Atmos. Environ.* 37, 5125–5133.
- Hay, K.L., Dearing, J.A., Baban, S.M.J., Loveland, P., 1997. A preliminary attempt to identify atmospherically-derived pollution particles in English topsoils from magnetic susceptibility measurements. *Phys. Chem. Earth.* 22, 207–210.
- Hu, X., Su, Y., Ye, R., Li, X., Zhang, G., 2007. Magnetic properties of the urban soils in Shanghai and their environmental implications. *Catena* 70, 428–436.
- Kim, W., Doh, S., Yu, Y., 2009. Anthropogenic contribution of magnetic particulates in urban roadside dust. *Atmos. Environ.* 43, 3137–3144.
- Lecoanet, H., L ev eque, F., Ambrosi, J., 2001. Magnetic properties of salt-marsh soils contaminated by iron industry emissions (southeast France). *J. Appl. Geophys.* 48, 67–81.
- Lecoanet, H., L ev eque, F., Ambrosi, J.P., 2003. Combination of magnetic parameters: an efficient way to discriminate soil-contamination sources (south France). *Environ. Pollut.* 122, 229–234.
- Lu, S.G., Bai, S.Q., 2006. Study on the correlation of magnetic properties and heavy metals content in urban soils of Hangzhou City, China. *J. Appl. Geophys.* 60, 1–12.
- Lu, S.G., Bai, S.Q., Xue, Q.F., 2007. Magnetic properties as indicators of heavy metals pollution in urban topsoils: a case study from the city of Luoyang, China. *Geophys. J. Int.* 171, 568–580.
- Łukasik, A., Szuszkiewicz, M., Magiera, T., 2014. Impact of artifacts on topsoil magnetic susceptibility enhancement in urban parks of the Upper Silesian conurbation datasets. *J. Soil Sediment.* 15, 1836–1846.
- Magiera, T., Zawadzki, J., 2007. Using of high-resolution topsoil magnetic screening for assessment of dust deposition: comparison of forest and arable soil datasets. *Environ. Monit. Assess.* 125, 19–28.
- Magiera, T., Strzyszc, Z., Kapicka, A., Petrovsky, E., 2006. Discrimination of lithogenic and anthropogenic influences on topsoil magnetic susceptibility in Central Europe. *Geoderma* 130, 299–311.
- Magiera, T., Strzyszc, Z., Rachwal, M., 2007. Mapping particulate pollution loads using soil magnetometry in urban forests in the Upper Silesia Industrial Region, Poland. *For. Ecol. Manag.* 248, 36–42.
- Magiera, T., Kapicka, A., Petrovsk, E., Strzyszc, Z., Fialov, H., Rachwal, M., 2008. Magnetic anomalies of forest soils in the upper Silesia-Northern Moravia region. *Environ. Pollut.* 156, 618–627.
- Maher, B.A., 1988. Magnetic properties of some synthetic sub-micron magnetites. *Geophys. J.* 94, 83–96.
- Moreno, E., Sagnotti, L., Dinar es-Turell, J., Winkler, A., Cascella, A., 2003. Biomonitoring of traffic air pollution in Rome using magnetic properties of tree leaves. *Atmos. Environ.* 37, 2967–2977.
- Morton-Bermea, O., Hernandez, E., Martinez-Pichardo, E., Soler-Arechalde, A.M., Santa-Cruz, R.L., Gonzalez-Hernandez, G., Beramendi-Orosco, L., Urrutia-Fucugauchi, J., 2009. Mexico City topsoils: heavy metals vs magnetic susceptibility. *Geoderma* 151, 121–125.
- Mullins, C.E., 1977. Magnetic susceptibility of the soil and its significance in soil science—a review. *J. Soil Sci.* 28, 223–246.
- Muxworthy, A.R., Schmidbauer, E., Petersen, N., 2002. Magnetic properties and Mömsbauer spectra of urban atmospheric particulate matter: a case study from Munich, Germany. *Geophys. J. Int.* 150, 558–570.
- Oldfield, F., Yu, L., 1994. The influence of particle size variations on the magnetic properties of sediments from the north-eastern Irish Sea. *Sedimentology* 41, 1093–1108.
- Pietrodangelo, A., Salzano, R., Rantica E. and Perrino, C., 2013. Characterisation of the local topsoil contribution to airborne particulate matter in the area of Rome (Italy). Source profiles. *Atmos. Environ.* 69, 1–14.
- Robertson, D.J., Taylor, K.G., Hoon, S.R., 2003. Geochemical and mineral magnetic characterisation of urban sediment particulates, Manchester, UK. *Appl. Geochem.* 18, 269–282.
- Sharma, A., Tripathi, B., 2008. Magnetic mapping of fly-ash pollution and heavy metals from soil samples around a point source in a dry tropical environment. *Environ. Monit. Assess.* 138, 31–39.
- Ska, M.J., Hasso-Agopsowicz, A., Kopcewicz, B., Sukhorada, A., Tyamina, K., Acedil, M.K., Ko-Hofmokl, D., Matviishina, Z., 2004. Magnetic properties of the profiles of polluted and non-polluted soils: a case study from Ukraine. *Geophys. J. Int.* 159, 104–116.
- Strzyszc, Z., Magiera, T., 1998. Magnetic susceptibility and heavy metals contamination in soils of Southern Poland. *Phys. Chem. Earth.* 23, 1127–1131.
- Thompson, R., Oldfield, F., 1986. *Environmental Magnetism*. Allen and Unwin, London.
- Walden, J., Oldfield, F., Smith, J., 1999. *Environmental Magnetism: A Practical Guide*. Quaternary Research Association, London.
- Wang, G., Xia, D., Liu, X., Chen, F., Yu, Y., Yang, L., Chen, J., Zhou, A., 2008. Spatial and temporal variation in magnetic properties of street dust in Lanzhou City, China. *Chin. Sci. Bull.* 53, 1913–1923.
- Wang, G., Oldfield, F., Xia, D.S., Chen, F.H., Liu, X.M., Zhang, W.G., 2012. Magnetic properties and correlation with heavy metals in urban street dust: a case study from the city of Lanzhou, China. *Atmos. Environ.* 46 (2), 289–298.
- Xie, S., Dearing, J.A., Boyle, J.F., Bloemendal, J., Morse, A.P., 2001. Association between magnetic properties and element concentrations of Liverpool street dust and its implications. *J. Appl. Geophys.* 48, 83–92.
- Yang, H., Xiong, H.G., Chen, X.G., 2014. Environmental magnetic properties and their spatial variability of topsoil in shihezi city. *Environ. Sci.* 35, 3537–3545.
- Zhang, C., Huang, B., Piper, J.D.A., Luo, R., 2008. Biomonitoring of atmospheric particulate matter using magnetic properties of *Salix matsudana* tree ring cores. *Sci. Total Environ.* 393, 177–190.